J Intell Robot Syst (2010) 59:283–298
DOI 10.1007/s10846-010-9403-1

Real-Time Seam Tracking Technology of Welding Robot with Visual Sensing

Hongyuan Shen · Tao Lin · Shanben Chen · Laiping Li

Received: 27 January 2007 / Accepted: 11 February 2010 / Published online: 8 June 2010

Abstract A seam tracking system with visual sensing free from calibration was developed for the robot applied in gas tungsten arc welding. A visual sensor with double-layer filter system was researched for the different levels of the welding current. An image processing in C++ language was developed to extract the seam trajectory and the offset of the torch to the seam in the welding images of aluminum alloys plates with grooves. The rectifying rule of the robot used in this paper was found based on the experimental data, and the seam tracking controller was also analyzed and constructed. The experimental results on straight line seam and curve seam demonstrated the efficiency of the proposal seam tracking system.

Keywords Visual sensing · Real time · Seam tracking · Welding robot

1 Introduction

Most of the welding robots applied in the automatic manufacture primarily work in "teach and playback" mode. Actually, welding encounters many variables, such as the errors of pre-machining, fitting workpiece and in-process thermal distortions, which would result in changes of the gap size and seam position. In welding process, such subtle changes would seriously affect the quality of the welding joint. The "teach and playback" robots cannot meet the requirement of quality and diversification. Therefore, it is obvious that real-time seam tracking is an important issue in this field.

H. Y. Shen (✉) · T. Lin · S. B. Chen
Institute of Welding Engineering, Shanghai Jiao Tong University, No. 1954 Hua Shan Road, Shanghai 200030, People's Republic of China
e-mail: Hongyuan.Shen@ge.com

L. P. Li
Shanghai Spaceflight Precision Machinery Research Institute, No. 76 Gui De Road, Shanghai 201600, People's Republic of China

The visual sensor has become the focus in the region of studying on the sensing technology of the welding robot because of its non-contact to the weld pool and abundant information. Most welding-related applications are used in welding seam tracking and weld pool checking [1–7].

A lot of previous researches have been done in the field of autonomous welding robot with visual sensing [8–12]. In some studies, the camera was directly used to view the weld pool and its vicinity to obtain control information, such as the size, the position of the weld pool, and the width of the seam gap [13, 14]. In other studies, the camera was used to view the laser stripe projected by a laser diode to detect the seam position, gap size, the offset, etc. [15–21]. However, most of the applications need the robot calibration, such as the coordinate systems, the end-effector position and the "hand-eye" calibration. The calibration is professional technology and quite complicated. Few operators can put the achievements into practice. Therefore, the seam tracking technology free-form robot calibration was proposed in this study.

In this paper, with the research background of the aeronautic manufacturing, the flange products, parts of a rocket, are welded using Motoman robot in Shanghai Spaceflight Precision Machinery Research Institute, China. The diameter of the flange made of LD 10 aluminum alloys is 148 mm, and the welding procedure is gas tungsten arc welding (GTAW) with BJ380A wire filler. When welding a circular workpiece, the start point of the seam must be re-welded for a good welding quality. Therefore, the end joint of the robot must circumrotate 400° at least. Due to the previously mentioned variables during the welding process, it is difficult for the robot to weld the flange along the seam center exactly, though it could be solved by the time-consuming method of teaching the robot at each position. Therefore, the seam tracking system using the visual sensing technology was developed for the robot to solve this problem.

In this study, the visual sensor viewed the weld pool and welding seam through the optical filters. An image processing algorithm was developed to extract the offset of the torch to the seam. A controller was developed for the seam tracking using the offset as the input parameter and the rectifying voltage as the output parameter. The image processing program and the tracking control program ran on a PC with the multithread programming technology in C++ language.

2 System Description

The vision-based welding robot system developed in this study consists of a visual sensor, a "teach and playback" robot, a rectifying function board, a welding power source, and a control computer. Figure 1 shows a schematic diagram of the real-time seam tracking system of welding robot with visual sensing. The robot is a six-axis industrial robot, made by Motoman Robot Co., Ltd (as shown in Fig. 2). It can be rectified in the vertical direction of welding through being set the voltage value (−10, +10 V) to a rectifying function board in the robot controller.

The visual sensor device is composed of charge-coupled device (CCD) camera and optical filter system. According to the spectral character of the aluminum alloy welding, a wideband filter and two dimmer glasses are used for the sensor. The transmission of the wideband is 590–710 nm. The attenuation of the two dimmer glasses is 99 and 70%, respectively. Figure 3a shows the prototype of the visual sensor

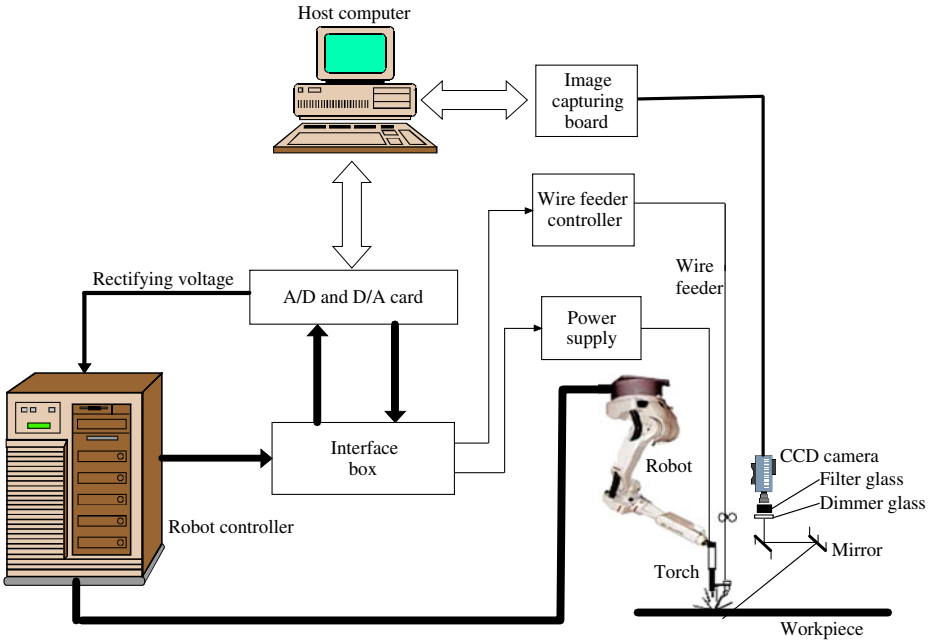

Fig. 1 The schematic diagram of the real-time seam tracking system of welding robot with visual sensing

Fig. 2 Robot welding system

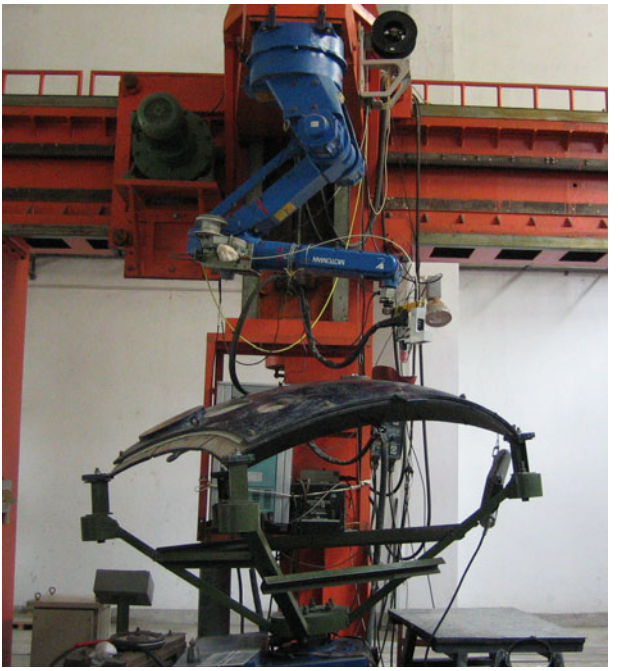

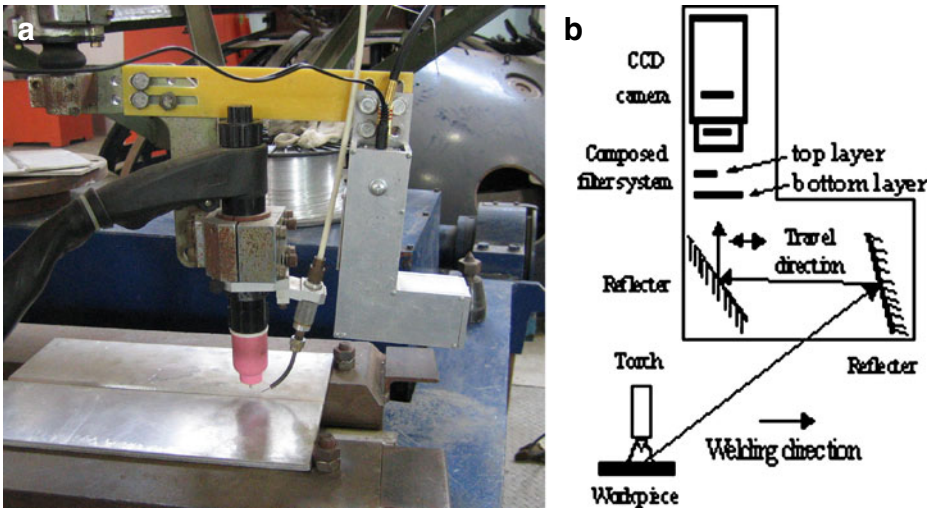

Fig. 3 The visual sensor device: **a** the prototype and **b** the structure

device. The CCD camera receives the welding pool image through the double-layer filter system after twice reflection, as shown in Fig. 3b. The double-layer filter system has been designed to accommodate the different light intensity between the weld pool and the seam. Figure 4 shows the compared results using single- and double-layer filter system. Figure 4a and b are the images captured with the single-layer filter system using the filters adapting to the weld pool and the seam, respectively. Compared with them, Fig. 4c is an obviously desirable image captured with the double-layer filter system using all selected glasses.

Figure 5 shows a block diagram of the software controller of the robot welding system based on an industrial computer. The computer captures the welding images through the visual sensor and the frame grabber, monitors the welding current and wire feed rate through the analog-digital converter board, sets the rectifying voltage (−10 and 10 V) through digital-analog converter board, detects the arc being or not through the digital input and output board. The computer runs the image processing program and data processing programs in respective threads. Figure 6 shows the program interface on computer screen during welding process.

3 Image Processing

The visual sensor is fixed on end joint of the robot to capture the welding images in the topface front direction. The sensor moves with the robot during the welding process, and the relative position of the torch and sensor is constant. Figure 7 is a GTAW image. The image processing technique that has been implemented is based upon 8-bit gray level image. This is combined with a simple calibration procedure that has been used to calculate the relation between the real distance (in the absolute coordinate system) and the image distance (in the image plane coordinate system).

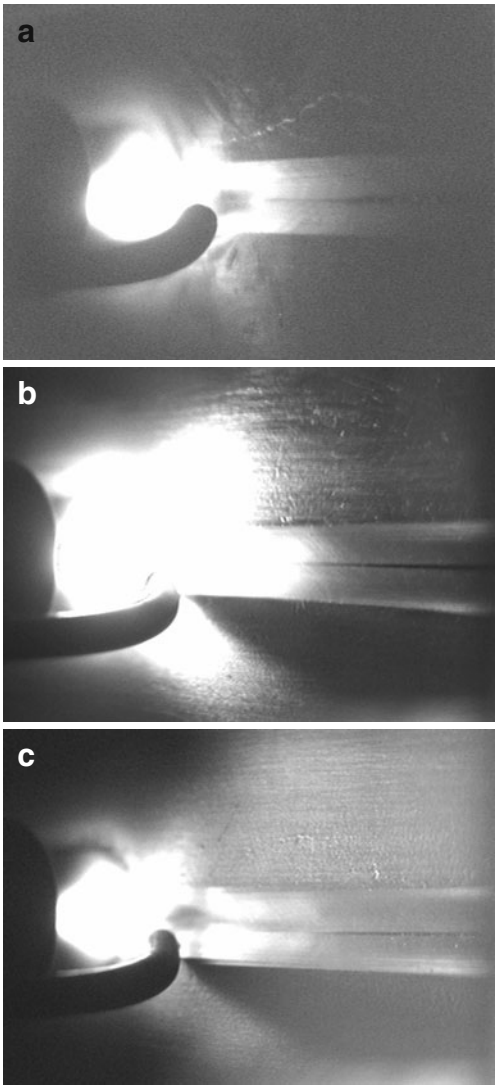

Fig. 4 The image with different filter system: **a** single-layer filter system with the wideband filter and the dimmer glass (99% attenuation); **b** single-layer filter system with the wideband filter and the dimmer glass (70% attenuation); and **c** double-layer filter system with the wideband filter and the dimmer glasses (99% and 70% attenuation)

Usually, the distance between the tip of the tungsten electrode and the surface of workpiece is 5 mm, which is appropriate to GTAW. A calibration plate with 5×5 mm panes is used to simulate the workpiece. When the distance between the tip of the tungsten electrode and the calibration plate is 5 mm and the tungsten electrode is normal to the calibration plate, an image is captured, as shown in Fig. 8. Point $O(0,0)$ is the projection point of the tungsten electrode on the calibration plate, it is defined as the original point of the calibration plate coordinate system. As the projection relationship, the deformation inevitably exists in the image plane coordinates system relative to the absolute coordinate system. It was found that the deformation of the abscissa and the ordinate both increase with the abscissa increasing, and the

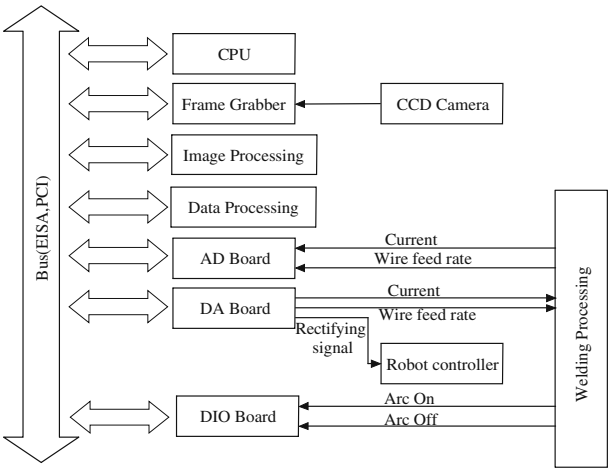

Fig. 5 Control system of the robot seam tracking

relation between the deformation and the abscissa is basically linear. Therefore, the deformations are supposed to be two linear relation represented as follows:

$$\begin{cases} f(n) = k \times n + b \\ f'(n) = k' \times n + b' \end{cases} \qquad n \geq 0 \tag{1}$$

where $f(n)$ and $f'(n)$ are the abscissa and the ordinate deformation with the abscissa increasing in the image plane coordinate system, respectively.

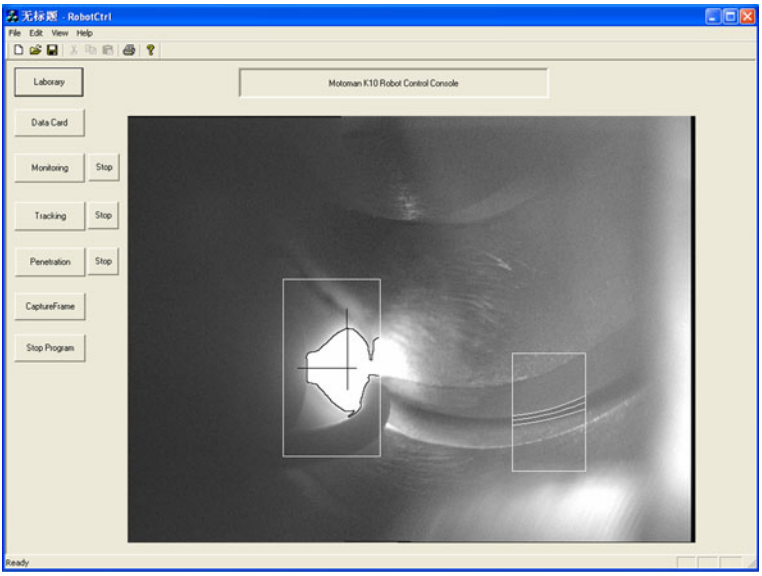

Fig. 6 The program interface during welding process

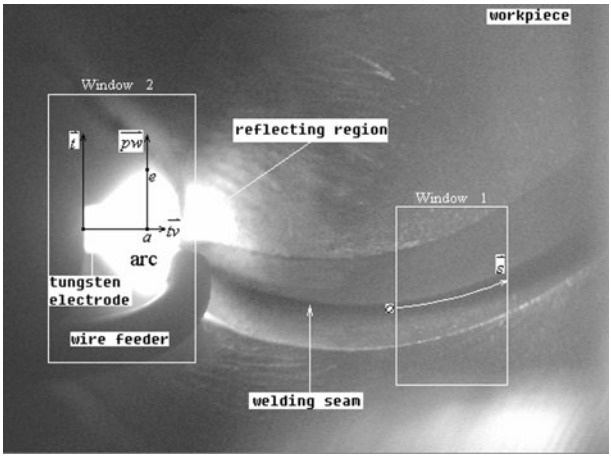

Fig. 7 The image of GTAW pool and seam

As a result, the relation of the image plane coordinates and the absolute coordinates can be worked out, which is given as follows:

$$\begin{cases} x_{\text{real}} = X\left(x_{\text{image}}\right) = \left\{-b + \left[b^2 - 4k\left(x_{\text{image\_o}} - x_{\text{image}}\right)\right]^{1/2}\right\} \times d_{\text{real}}/2k \\ y_{\text{real}} = Y\left(y_{\text{image},} X\left(x_{\text{image}}\right)\right) = \left(y_{\text{image\_o}} - y_{\text{image}}\right) \times d_{\text{real}} 2 \Big/ \left(x_{\text{real}} \times k' + d_{\text{real}} \times b'\right) \end{cases} \tag{2}$$

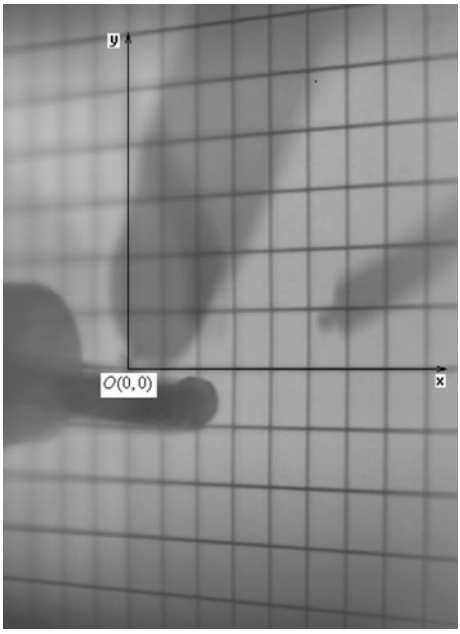

Fig. 8 The picture of CCD calibration

where $(x_{\text{image}}, y_{\text{image}})$ and $(x_{\text{real}}, y_{\text{real}})$ are the image plane coordinates and the absolute coordinates, respectively. $(x_{\text{image\_o}}, y_{\text{image\_o}})$ is the coordinate of point $O(0,0)$ in the image plane coordinate system, d_{real} is the interval of the panes, and X and Y are the abscissa and the ordinate relation function between the image plane coordinates and the absolute coordinates, respectively.

Actually, as the arc light is too intense to clearly view the seam near the weld pool, the current offset of the torch to the seam is defined as the offset at the center of weld pool, which is calculated by fitting the function of the seam center. Figure 9 shows the offset in the image plane coordinate system. Point a is the center of the weld pool, d is the offset, and $f_3(x)$ is the fitted seam center function. Figure 9 can be understood better combined with Fig. 7.

Since most of the captured 768- × 576-pixel image is useless for seam tracking and will cost plenty of CPU time, the authors selected two areas for image processing, called Windows 1 and 2 (shown in Fig. 7), respectively.

The seam center and the center of the weld pool have been exacted accurately by a series of digital image processing procedures in the image plane coordinate system. In Window 1, the image processing sequence is as follows: median filter, detecting Robert operator edge, thresholding, removing small area, thinning, extracting the seam edges, fitting edges with least square method, and calculating the seam center. The image processing results of Window 1 are shown in Fig. 10.

Figure 10g is the result after the digital image processing. Then, both seam edges are fitted by nonlinear least square method (as shown in Fig. 10h). The edges curve is expressed as

$$\begin{cases} f_1(x) = a_1 x^2 + b_1 x + c_1 \\ f_2(x) = a2x^2 + b_2 x + c_2 \end{cases} \tag{3}$$

where $f_1(x)$ and $f_2(x)$ are the seam up-edge function and the seam down-edge function, respectively.

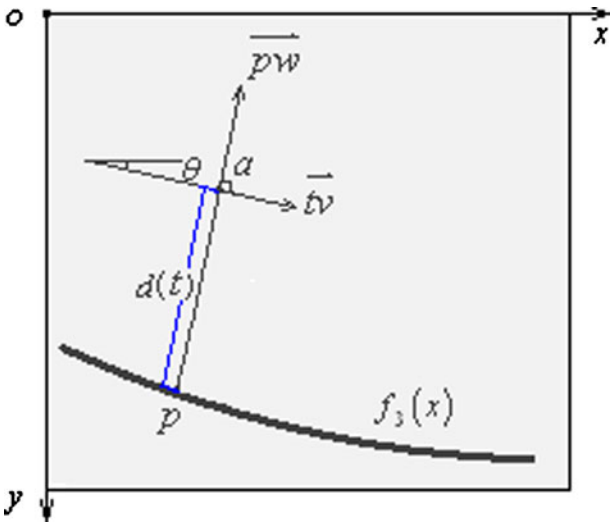

Fig. 9 The offset of the torch to the seam in the image plane coordinate system

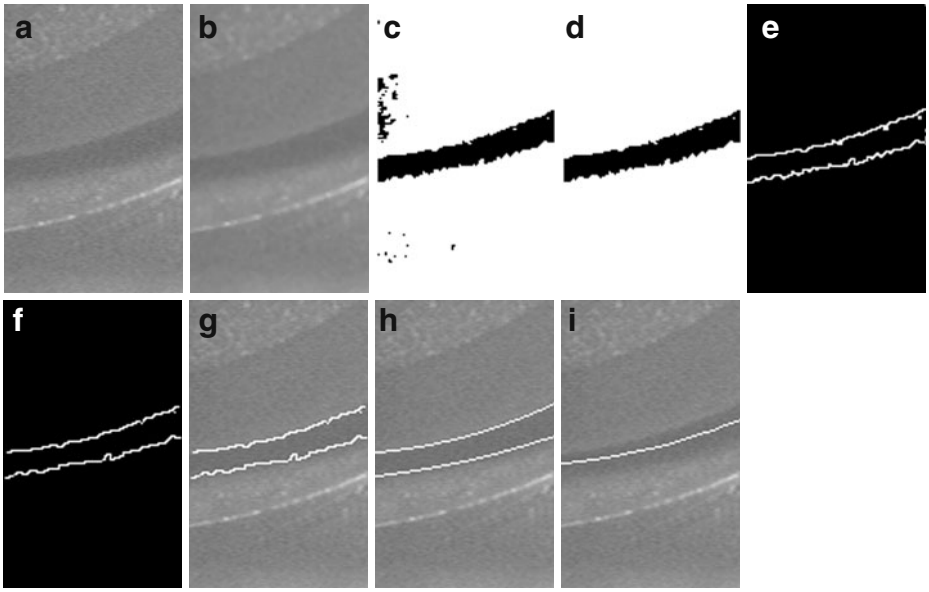

Fig. 10 Image processing of Window 1: **a** original image, **b** the filtered image by a median filter, **c** the image with threshold value chosen to be 125, **d** the image after removing small area, **e** the image detected using Roberts operator, **f** the image after skeleton thinning, **g** the welding seam points on original image, **h** the welding seam edge points fitted by nonlinear least square method, and **i** the welding seam center

Therefore, the seam center function $f_3(x)$ is represented as follows:

$$f_3(x) = \left[f_1(x) + f_2(x)\right]/2 \tag{4}$$

Compared with Window 1, the image processing of Window 2 is similar. The sequence is as follows: median filter, thresholding, detecting Robert operator edge, thinning, and extracting the outline of the arc and center of the weld pool. The image processing results of Window 2 are shown in Fig. 11.

In Fig. 11g, the orientation of the tungsten electrode ($\overline{tv}$) is then expressed as:

$$f(x) = kx + b \tag{5}$$

Then, the rate of grade of line $\overline{pw}$ is $-\frac{1}{k}$ and point e, where the arc is the widest, is on line $\overline{pw}$. Therefore, line $\overline{pw}$ is as follows:

$$f'(x) = -\frac{1}{k}x + b' \tag{6}$$

By calculating Eqs. 5 and 6, the coordinates of point a is represented as:

$$\begin{cases} a_x = \left[\left(b' - b\right)k\right]/\left[k^2 + 1\right] \\ a_y = \left[k^2 b' + b\right]/\left[k^2 + 1\right] \end{cases} \tag{7}$$

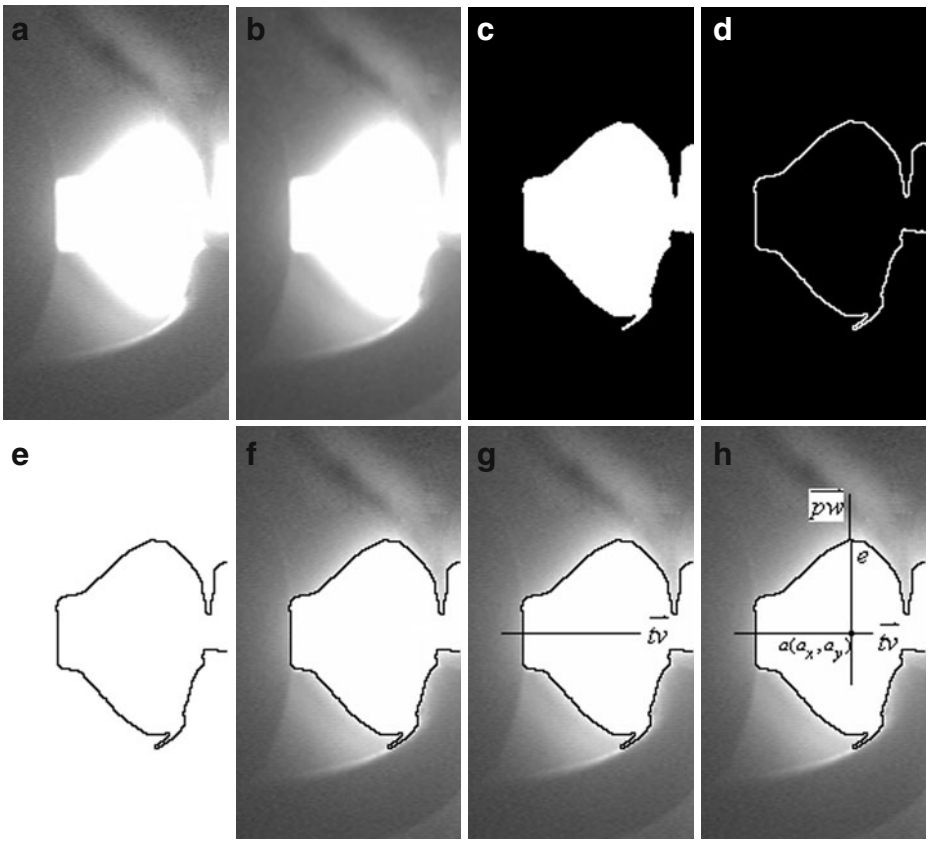

Fig. 11 Image processing of Window 2: **a** original image, **b** the filtered image by a median filter, **c** the image with threshold value chosen to be 250, **d** the image detected using Roberts operator, **e** the image after skeleton thinning, **f** the arc outline on original image, **g** the orientation of the tungsten electrode, and **h** the projection point of the tip of torch

According to Eqs. 2 and 7, the real offset d_{real} is given as follows:

$$d_{\text{real}} = \left\{ \left[X\left(a_x\right) - X\left(p_x\right) \right]^2 + \left[Y\left[a_{y,} X\left(a_x\right) \right] - Y\left[p_{y,} X\left(p_x\right) \right] \right]^2 \right\}^{1/2} \tag{8}$$

where (p_x, p_y) is the coordinate of point p (shown in Fig. 9).

This image processing algorithm proposed above has been validated and demonstrated that it can cope with images when welding with the different current (in the range of 150–340A), which is usually used for making welds in medium plate aluminum alloy weld (in the range of 3–8 mm). The accuracy of the measurement is in the range of ±0.1 mm.

4 Seam Tracking Controller

As the rectifying rule of the robot is not open to public, a flat butt welding experiment is designed in order to find the rectifying rule and build the controller, as shown in

Fig. 12. *ae* is the seam line, and *abcde* is the taught trajectory at the beginning. It was found that if the robot could weld the workpiece with the tracking control along *af* exactly, the robot would automatically translate the taught trajectory to be *fd′e* instead of *fde*. For the same reason, *ge″* would be the taught trajectory instead of ge′. Therefore, a negative trend of the offset exits in *af* and *ge* stages, and a positive trend of the offset exits in *fg* stage if the robot could weld along *ae* exactly in this experiment.

According to the analysis, the different voltages, such as 1, 1.5, 2, and 3 V, are used to track the workpiece designed in Fig. 12. Figure 13 shows the offset curves checked using the sensor. When the rectifying voltage is 1 V, the rectifying speed is so small that the robot cannot weld along *ae*; especially in *fg* stage, the offset is so large that the seam is outside the scope of Window 1, and the computer obtains wrong results. When the rectifying voltage is 1.5 V, the offset curve has the same trend as Fig. 12c, which proves that the voltage is still small. When it is 2 V, the offset curve fluctuates at the vicinity of zero. Obviously, 2 V is an adaptive rectifying voltage for this seam. When it is 3 V, the fluctuation of the curve is too large and is worse than that of 2 V. Therefore, we came to a conclusion that the different offset must be corresponding with an adaptive rectifying voltage.

Therefore, a simple proportional–integral–derivative controller has been constructed after lots of the experiments. The offset is the input parameter, and the rectifying voltage is the output parameter. It is given in Eq. 9.

$$v(k) = k_{\mathrm{p}} e(k) + k_{\mathrm{i}} \sum_{j=0}^{k} e(j) + k_{\mathrm{d}} \left[e(k) - e(k-1) \right] \tag{9}$$

where $v(k)$ is the rectifying voltage, $e(k)$ is the offset, k_{p} is the proportional gain, k_{i} is the integral gain and k_{d} is the derivative gain.

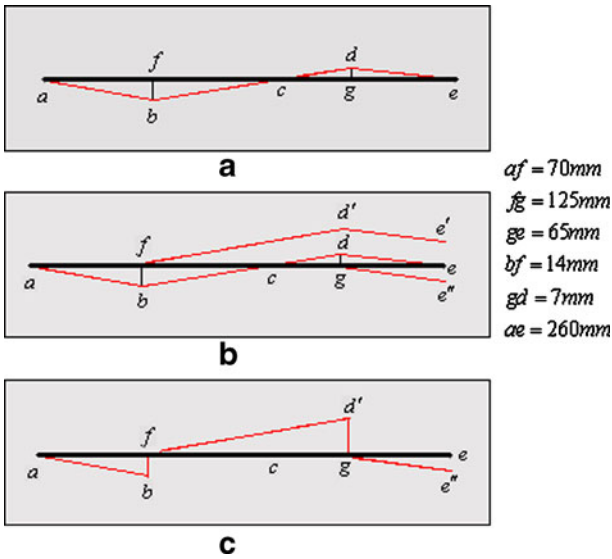

Fig. 12 The robot welding trajectory: **a** the taught trajectory, **b** robot trajectory at different time, and **c** the trend of the offset at different stage

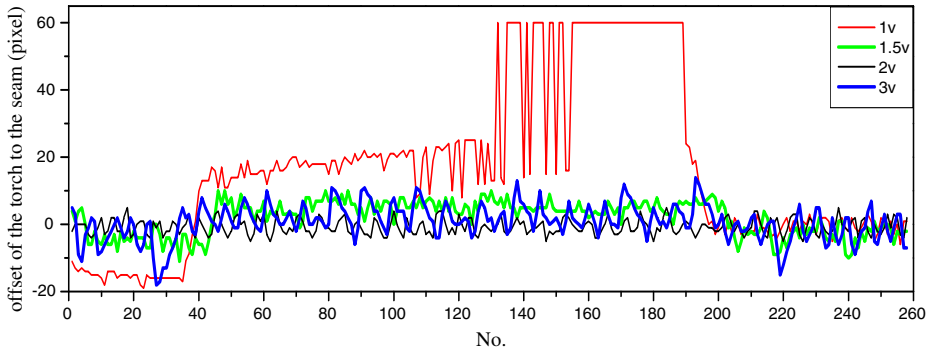

Fig. 13 Comparison between different rectifying voltages

The period of the tracking control is 400 ms using an industrial computer with Pβ 1.7 GHz CPU and 512 M memory. In a period, the offset of the torch to the seam is extracted one time, and the rectifying voltage is updated one time.

5 Experiment Results

Welding experiments are conducted with GTAW for the arc welding robot system to evaluate the feasibility of real-time tracking control during the backing weld process. Two types of welding seam, straight line designed in Fig. 12 and curve line shown in Fig. 14, are chosen for the seam tracking. The specific parameters are given in Table 1.

Figure 15 shows two pictures illustrating the result of the welding experiment of the straight line seam with or without the tracking control, respectively. Figure 15a

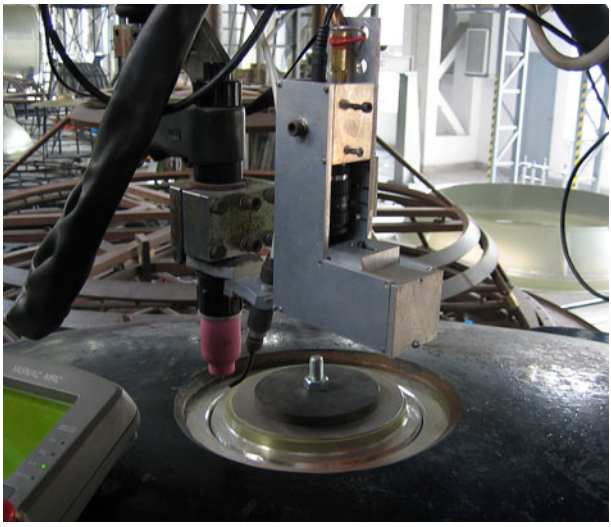

Fig. 14 The flange product (Φ148 mm)

Table 1 The specific experiment parameters

Parameter	Value
Process	AC GTAW at 60 Hz
Material	6-mm thick LD 10 aluminum alloy with a Y-groove of 80°
Thickness of root face	2 mm
Backing bar	1Cr18Ni9Ti
Welding current	255 A
Wire feed rate and the wire type	20.10 mm s^{-1} BJ380A Φ1.6 mm
Welding speed	2.67 mm s^{-1}
Shielding gas	Ar

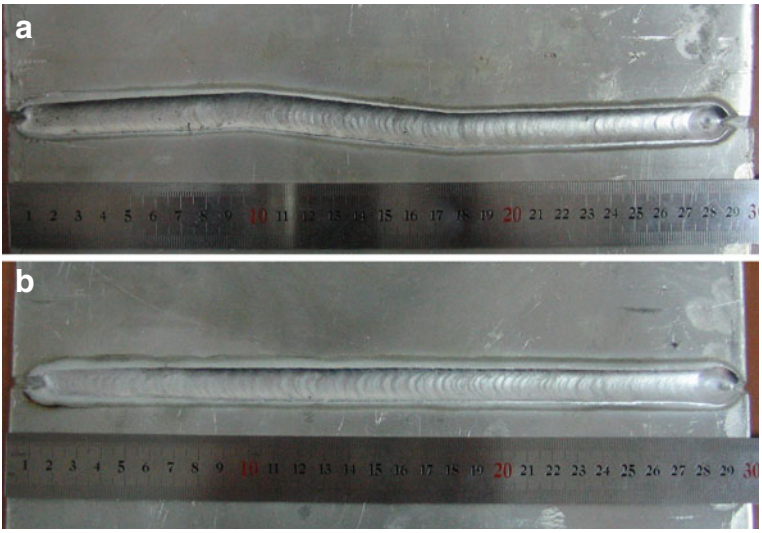

Fig. 15 Comparison picture of the backing weld with tracking control or without tracking control: **a** with tracking control and **b** without tracking control

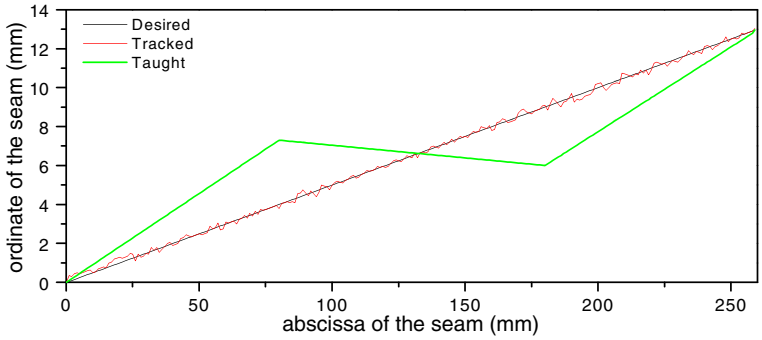

Fig. 16 The offset error of the straight line seam with tracking control

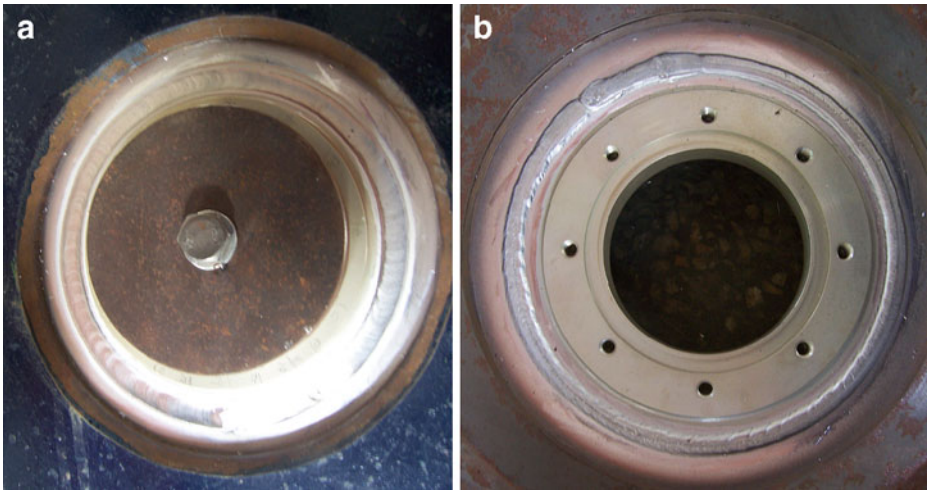

Fig. 17 The backing weld of the flange with seam tracking: **a** topface and **b** underside

shows the welding result for the preset trajectory without tracking control. Figure 15b shows the result for the same preset trajectory with tracking control. The offset error is in the range of ±0.3 mm, and the result is shown in Fig. 16.

An initial offset from 0 to 2 or −2 mm is preset along the circle seam by teaching the robot in the flange welding experiment. Figure 17 shows a favorable result in topface and underside of the flange, and Fig. 18 shows the offset error that is in the range of ±0.5 mm.

Fig. 18 The offset error of the flange seam with tracking control

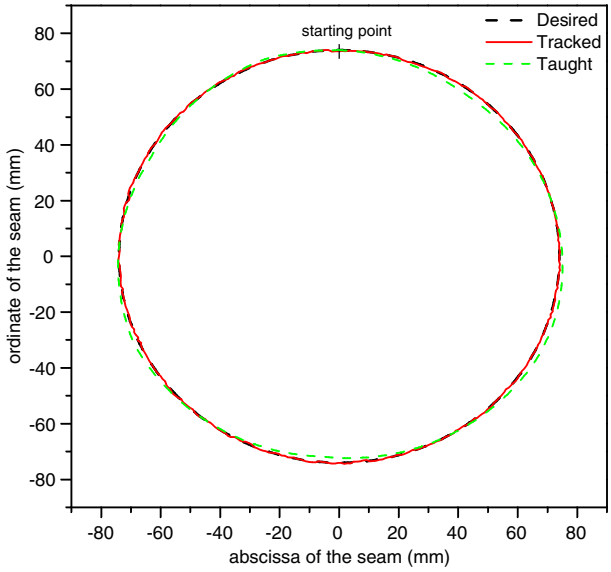

According to these results, it can be assured for the real-time seam tracking system to be very feasible to control the offset for the different productions.

6 Conclusion

In this paper, the real-time seam tracking system of welding robot with visual sensing was presented, which demonstrated a successful seam tracking technology for "teach and playback" robot free from robot calibration. The computer could capture the clear welding image in different levels of welding current using the proposed visual sensor device with the double-layer filter system. The reliable detection of the seam could be achieved by the proposed image processing algorithms based on the welding image. The tracking controller could accurately track straight line and curve line seam, and the accuracy of the tracking system was in the range of ± 0.3 mm for straight line seam and ± 0.5 mm for the flange product of the rocket. At present, the proposed system has been applied in practice.

Improvement should be made in optical filters and the image analysis algorithm to deal with the images in other welding procedures, such as MIG/MAG in the future work. Another CCD camera should be added to view the weld pool from its rear to obtain more information of the weld pool for a penetration control.

Acknowledgements This work is supported by the National Natural Science Foundation of China under grant no. 50575144. The authors wish to thank the anonymous reviewers for their valuable comments on the earlier draft of this paper.

References

1. Yu, J-Y., Na, S-J.: A study on vision sensors for seam tracking of height-varying weldment, part 1: mathematical model. Mechatronics **7**(7), 599–612 (1997)
2. Yu, J-Y., Na, S-J.: A study on vision sensors for seam tracking of height-varying weldment, part 2: applications. Mechatronics **8**(1), 21–36 (1998)
3. Bauchspiess, A., Absi Alfaro, S.C., Dobrzanski, L.A.: Predictive sensor guided robotic manipulators in automated welding cells. J. Mater. Process. Technol. **109**, 13–19 (2001)
4. Smith, J.S., Balfour, C.: Real-time top-face vision based control of weld pool size. Ind. Rob. **32**(4), 334–340 (2005)
5. Zhou, L., Lin, T., Chen, S.B.: Autonomous acquisition of seam coordinates for arc welding robot based on visual servoing. J. Intell. Robot. Syst. **47**, 239–255 (2006)
6. http://www.meta-mvs.com
7. Lee, S.K., Na, S.J.: A study on automatic seam tracking in pulsed laser edge welding by using a vision sensor without an auxiliary light source. J. Manuf. Syst. **21**(4), 302–315 (2002)
8. Kim, J.S., Son, Y.T., Cho, H.S., Koh, K.I.: A robust method for vision-based seam tracking in robotic arc welding. Mechatronics **6**(2), 141–163 (1996)
9. Kuo, H-C., Wu, L-J.: An image tracking system for welded seams using fuzzy logic. J. Mater. Process. Technol. **120**(1), 169–185 (2000)
10. Bae, K.Y., Lee, T.H., Ahn, K.C.: An optical sensing system for seam tracking and weld pool control in gas metal arc welding of steel pipe. J. Mater. Process. Technol. **120**(2), 458–465 (2002)
11. Ge, J., Zhu, Z., He, D., Chen, L.: A vision-based algorithm for seam detection in a PAW process for large-diameter stainless steel pipes. Int. J. Adv. Manuf. Technol. **26**(10), 1006–1011 (2005)
12. Roboics Online. http://www.roboticsonline.com/public/articles/archivedetails.cfm?id=605
13. Yamane, S., Kaneko, Y., Kitahara, N., Ohshima, K., Yamamoto, M.: Neural network and fuzzy control of weld pool with welding robot. In: Ind. Appl. Soc. Annu. Meet. Conf. Rec. 1993, IEEE, vol. 3, pp. 2175–2180 (1993)

14. Zhao, D.B., Chen, S.B., Wu, L., Dai, M., Chen, Q.: Intelligent control for the shape of the weld pool in pulsed GTAW with filler metal. Weld. J. **80**(11), 253–260 (2001)
15. Smith, J.S., Lucas, J.: Vision-based seam tracker for butt-plate TIG welding. J. Phys., E Sci. Instrum. **22**(9), 739–744 (1989)
16. Luo, H.: Robotic welding, intelligence and automation, laser visual sensing and process control in robotic arc welding of titanium alloys. LNCIS **299**, 110–122 (2004)
17. Meta-Scout GmbH. http://www.scout-sensor.com/
18. Lee, S.K., Chang, W.S., Yoo, W.S., Na, S.J.: A study on a vision sensor based laser welding system for bellows. J. Manuf. Syst. **19**(4), 249–255 (2007)
19. OMSMI. http://lca.kaist.ac.kr/Researches/
20. BARA. http://www.bara.org.uk/pressreleases/meta2.htm
21. Seam-tracking, guidance systems. http://www.manufacturingtalk.com/indexes/categorybrowseei.html